Int. J. Electrochem. Sci., 11 **(2016)** 6501 – 6513, doi: 10.20964/2016.08.59

International Journal of
ELECTROCHEMICAL
SCIENCE
www.electrochemsci.org

Inhibition of Microbial Pyrite Oxidation by PropS-SH for the Control of Acid Mine Drainage

Zan Luo[1], *Yun Liu*[1,*], *Runliang Zhu*[2],*Xin Hu*[1]

[1] Department of Environmental Science and Engineering, Xiangtan University, Xiangtan 411105, China
[2] Key Labortory of Mineralogyand Metallogeny, Guangdong Provincial Key Laboratory of Mineral Physics and Material Research & Development, Guangzhou Institute of Geochemistry, Chinese Academy of Sciences, Guangzhou 510640, China
[*]E-mail: liuyunscut@163.com

Received: 6 May 2016 / *Accepted:* 21 June 2016 / *Published:* 7 July 2016

Acidithiobacillus ferrooxidans, an acidophilic sulfur and iron-oxidizing microorganism, plays an important role in the oxidation of FeS_2 and the formation of acid mine drainage (AMD). In this study, the stability of γ-mercaptopropyltrimethoxysilane(PropS-SH) treated pyrite in the presence of *Acidithiobacillus ferrooxidans* was investigated by electrochemical techniques in conjunction with bioleaching approach. In addition, the chemical and morphological characteristics of pyrite before and after coated by PropS-SH were analyzed with X-ray photoelectron spectrometer (XPS) and contact angle tests. The results from electrochemical tests indicated that the coating of PropS-SH significantly decreased electrochemical activity of pyrite in bioleaching solutions. The results of bioleaching experiments showed that PropS-SH coating could effectively suppress the release of S and Fe species from pyrite and inhibit the growth of bacteria. These results were attributed to the formation of a hydrophobic layer on pyrite surface by chemisorption of PropS-SH which could limite the contact of bacteria with pyrite.

Keywords: pyrite; Acid mine drainage; inhibition; *Acidithiobacillus ferrooxidans*; γ-mercaptopropyltrimethoxysilane (PropS-SH); Electrochemical technique.

1. INTRODUCTION

Pyrite (FeS_2) is frequently present in waste rock dumps, tailings, ores and coal deposits[1]. Natural oxidation of pyrite, especially catalyzed by iron-oxidizing bacteria such as *Acidithiobacillus ferrooxidans*, results in the formation of acid mine drainage (AMD)[2-4]. AMD is often characterized by low pH water with high concentration of heavy metals. Hence, AMD is a serious problem in many areas with mining [5].

In the last few decades, several strategies for the source control of AMD have been developed[6]. The most common approach involves the passivation of pyrite, in which a protective coating is formed on the surface of pyrite to prevent it from contacting the air, water and other oxidants[7, 8]. To date, several types of passivation agents have been proposed including phosphate[9, 10], silicate[11], phospholipids[12, 13], humic acids[14], 8-hydroxyquinoline[15], triethylenetetramine(TETA)[16, 17] and sodium triethylenetetramine-bisdithiocarbamate (DTC-TETA)[18]. These passivation agents have been found to be effective in inhibiting pyrite oxidation, but each of these passivation agents has their own defects, For example, the formation of phosphate, silicate and 8-Hydroxyquinoline coatings involve the use of H_2O_2, which seriously limit their use in practical fields. Some other passivation agents including TETA and DTC-TETA are toxic to the environment. Therefore, it is imperative to explore more environmentally friendly alternatives.

Recently, our laboratory has found three kinds of harmless and environmentally friendly coating agents γ-mercaptopropyltrimethoxysilane (PropS-SH), γ-minopropyltrimethoxysilane (APS) and vinyltrimethoxysilane(VTMS) could retard chemical oxidation of pyrite effectively, and PropS-SH shows the highest inhibition efficiency[19]. However, the capability of PropS-SH to passivate pyrite in the presence of microorganisms like *Acidithiobacillus ferrooxidans*, which plays an important role and is unavoidable in AMD formation, is unknown. Additionally, the mechanism of pyrite oxidation suppression by PropS-SH coating is still poorly understood. To increase knowledge on this subject, more fundamental studies on the stability of PropS-SH treated pyrite in the presence of *Acidithiobacillus ferrooxidans* and the nature of the coated pyrite surface are required. To meet this objective, a preparatory assessment of inhibitory efficiency for PropS-SH coating during pyrite bioleaching process was provided by using electrochemical tests, such as tafel polarization, cyclic voltammetry (CV) and electrochemical impedance spectroscopy (EIS). Electrochemical techniques are useful tools to analyze the biochemical processes occurring in the pyrite/culture medium interface. Traditional biological leaching tests were also applied to further confirm the effect of PropS-SH coating on the speed of pyrite biological oxidation. In addition, the chemical and morphological characteristics of pyrite before and after coated by PropS-SH were analyzed with XPS and contact angle test.

2. EXPERIMENTAL

2.1. Materials preparation

Pyrite used in this study was obtained from ChangSha Mineral market. The chemical composition analyzed by X-ray fluorescence (XRF) showed that the purity of pyrite was 99.56% and the main impurity was Al_2O_3(0.35%). Samples of pyrite were cut into cubes with side length of 1 cm and polished sequentially into mirror-like surface with waterproof abrasive paper. To eliminate impurities the samplies were rinsed with ultrapure water and acetone. The remaining samples were crushed and screened to collect the particles with diameter less than 75μm. The processed feed samples were then stored in a vacuum desiccator before using.

2.2. Coating processing

The coating agents were prepared by adding various volumes of PropS-SH to a mixture of ultrapure water and ethanol (the volume ratio of PropS-SH /ultrapure water/ethanol were 1/1/98, 3/3/94, and 5/5/90 for 1%, 3%, and 5% PropS-SH agents, respectively). The initial pH of the solutions was adjusted to 4.0 with 0.1M HCl. These coating agents were stirred for 60 min at 40℃ and then pyrite samples prepared previously were dissolved in the coating solutions. The solutions were kept stirring for 120 min at 50℃ after adjusting the pH to 9 with 0.5 M ammonium hydroxide. The coated pyrite was separated from solutions by filtration and dried at 100℃ for 12h. All reagents used in the experiment were of analytical grade and ultrapure water was used to prepare solutions.

2.3 Bacterial strain and growth conditions

Acidithiobacillus ferrooxidans (Accession number of 16S rDNA in GeneBank:GQ984157) used in this work were isolated from Dabaoshan sulfur-polymetallic mines in Guangdong, China[20]. Before the experiments, *Acidithiobacillus ferrooxidans* were cultivated in 9K medium replacing the ferrous sulfate with 5% w/v pyrite as the sole energy source at pH 2. The bacterial strains used in the tests were adapted to the pyrite concentrate by being continuously subcultured over a year.

2.4 Electrochemical measurements

A standard electrochemical system with three electrodes was used. The working electrode of coated or uncoated pyrite was assembled in our laboratory by a method pulished elsewhere[19]. The counter electrode was a Pt foil (15 mm×15 mm) and the reference electrode was a saturated calomel electrode (SCE) placed in a Luggin's capillary. The electrochemical cell was charged with 200 ml 9K medium inoculated with *Acidithiobacillus ferrooxidans*. All the electrochemical tests were carried out when the bacteria reached the logarithmic growth period.

The electrochemical measurements were performed at CHI 660 Electrochemical Workstation and all potentials quoted in this paper were referenced to the SCE. Cyclic voltammetry tests were conducted at a sweep rate of 50 mV/s and the scan ranged from -0.6V/SCE to +0.8V/SCE. Tafel polarization curves were measured over the range of open circuit potential (OCP) ±0.2V/SCE at a scan rate of 1 mV/s. The impedance spectra were obtained at OCPs. The frequency range was from 10,000 to 0.01Hz with the AC signal amplitude of 10mV. The impedance data were analyzed by using ZSimpWin 3.00 software.

2.5 Biological leaching experiments

For bioleaching experiments, *Acidithiobacillus ferrooxidans* cells were inoculated into 250-mL flasks containing 100 mL of sterilized culture medium and 1g of uncoated or coated pyrite with different concentration of PropS-SH. The initial pH and cells concentration were 2 and 2.5×10^7

cell/mL , respectively. The flasks were kept for shaking on a rotary shaker at 150 rpm at 30℃.

Periodically, solution samples were assayed for pH, total Fe, SO_4^{2-} and cell concentration. The pH value of the leaching solution was analyzed by a waterproof hand-held pH/mV meter (Eutech instruments pH 310, USA). Total Fe of the leaching solution was determined by o-phenanthroline spectrophotography (UV-752N, Shanghai Analytical Instrument Co. Ltd., China) and the absorbance reading was taken at 510 nm. SO_4^{2-} concentration of the leachate was analyzed by the baryta yellow spectrophotometric method. The cell density was determined by direct counting with a blood corpuscle counter (XB-K−25), Triplicate leach experiments were performed under identical conditions.

2.6 Methods of analysis

The XPS analysis of the coated and uncoated pyrite were performed on a Thermo Scientific Escalab 250 X-ray spectrometer using a monochromatic Al Kα source (1486.8eV). Contact angles were measured with a Rame-Hart Model 250 goniometer using the sessile drop method. Drops of 8μl deionized filtered water were deposited with a microsyringe on the surfaces of materials, and the contact angles were measured after a defined period of time in order to allow the establishment of equilibrium.

3. RESULTS AND DISCUSSION

3.1. Electrochemical tests

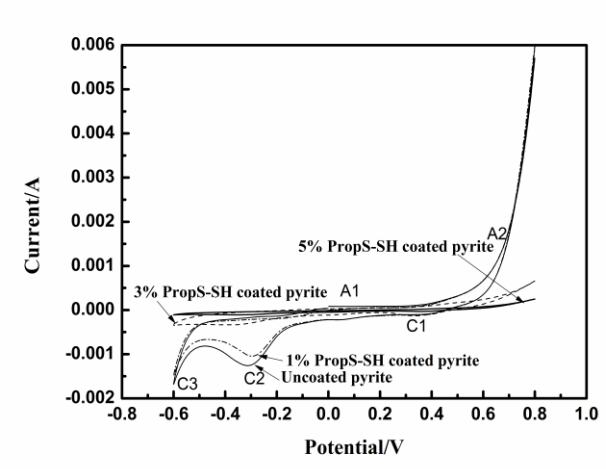

Figure 1. Cyclic voltammetry curves of uncoated,1% , 3% and 5% PropS-SH coated pyrite electrodes in bioleaching solutions.

Figure 1 shows the cyclic voltammetric curves obtanined for uncoated and coated pyrite electrodes immersed in bioleaching solutions. In the anodic scan of these curves, two oxidation peaks

are observed. A_1 is attributed to the oxidation of pyrite to S_0. When the potential is larger than 0.5 V, the dissolution of superficial S_0 (product of reaction A_1) is expected to occur contributing to the appearance of the anodic current peak A_2[21]. In the reverse direction, the ferric iron that accumulated on the pyrite surface during the anodic scan become reduced back to ferrous iron which produces the cathodic current peak C_1. At approximately -0.3V, a signal of C_2 is observed, which can be interpreted as two possible reactions: (1) the reduction of S_0 formed during the anodic scan, and (2) the reduction of FeS_2 to form FeS and H_2S. When the potential become more negative, the evolution of hydrogen could be observed, corresponding to the reduction peak C_3.

Comparing the Cyclic voltammetry curves of pyrite electrodes coated by PropS-SH of concentration between 0% and 5%, the anodic and cathodic current peaks are decreased with an increase in PropS-SH. When 5% PropS-SH is adopted in the coating treatment, the anodic and cathodic current peaks are too weak to be detected. This indicats that the protective layer of PropS-SH can inhibit the microbial leaching of pyrite and inhibition efficiency is increased with the increase of PropS-SH.

The Tafel polarization curves of pyrite electrodes pretreated with various concentrations of PropS-SH in bioleaching solutions are presented in Fig.2.

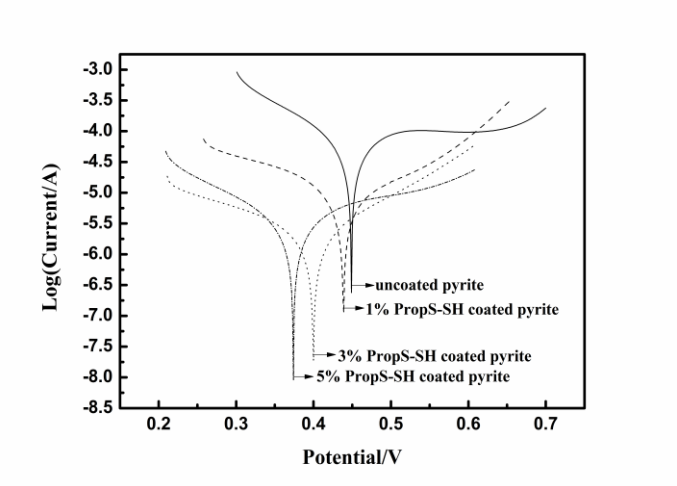

Figure 2. Tafel polarization curves of uncoated , 1% , 3% and 5% PropS-SH coated pyrite electrodes in bioleaching solutions.

Table 1. Tafel polarization parameters for uncoated and coated pyrite electrodes with different concentrations of PropS-SH in bioleaching solutions.

PropS-SH concentrations	E_{corr} (mV / SCE)	β_c (m*V* /decade)	β_a (m*V* /decade)	j_{corr} (μA cm^{-2})
Bare pyrite	449	142.71	3861.00	136.61
1%	439	165.95	244.68	13.72
3%	400	182.58	225.18	4.798
5%	374	226.19	147.84	2.871

The corrosion kinetic parameters including corrosion potential (E_{corr}) and corrosion current density (I_{corr}) deduced from the curves are given in Table 1.

It can be seen that the corrosion current density value decreases from 136.61 mA/cm^2 for the bare pyrite electrode to 13.72, 4.798 and 2.871 mA/cm^2, respectively, for the coated pyrite electrodes with 1%, 3% and 5% PropS-SH. As in the case of Cyclic voltammetry measurements, the increase in concentration of the inhibitor decreases the rate of pyrite oxidation in the presence of *Acidithiobacillus ferrooxidans.* The decrease in the pyrite oxidation decreases the oxide (e.g., iron ions) on the pyrite electrode surface, thus also resulting in the reduced E_{corr}value.

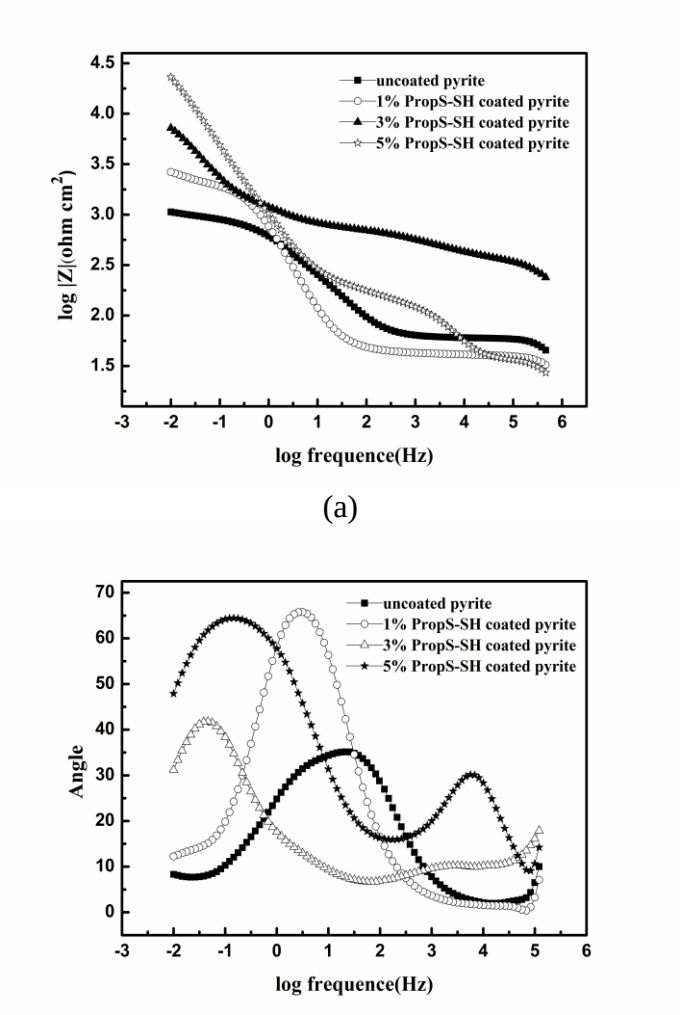

Figure 3. The impedance (a) and phase angle (b) Bode plots measured with uncoated , 1% , 3% and 5% PropS-SH coated pyrite electrodes in bioleaching solutions.

Fig. 3 displays the impedance (a) and phase angle (b) Bode plots measured with pyrite electrodes containing different concentrations of PropS-SH in bioleaching solutions. Corrosion resistance of pyrite electrodes can be quantitatively evaluated by the low-frequency impedance values (Z_{lf})[22]. It is shown from Fig. 3(a) that as the PropS-SH concentration increases, Z_{lf} values for pyrite electrodes increase. The phenomenon can be understood as following: increasing the PropS-SH

concentration, more and more molecules adsorb on the pyrite surface and form a denser film gradually.

Fig. 3(b) shows that only one capacitive loop is observed in the impedance spectra of bare and 1% PropS-SH coated pyrite electrode. This indicates that, in the absence or low concentration of inhibitor, pyrite oxidation rate is mainly controlled by a charge transfer process. In contrast, at least two capacitive loops can be distinguished in the spectra of coated pyrite electrodes with 3% and 5% PropS-SH, suggesting that there is an additional electrochemical process other than the dissolution of pyrite. The time constant in the low-frequency region is related to the charge-transfer resistance of pyrite oxidation, while the time constant corresponding to the high-frequency loop usually represents the response of coating, thus exhibits the coatings characteristics and performance in the solution[23]. The appearance of the high-frequency loop reflects that a PropS-SH film is formed on the surface of pyrite. It is worth noting that the diameter of the capacitive semicircle for pyrite electrode coated with 5% PropS-SH is much larger than that for 3% PropS-SH, that is, the thickness of the coating film increases with the increase of PropS-SH concentration.

3.2. Biological leaching test

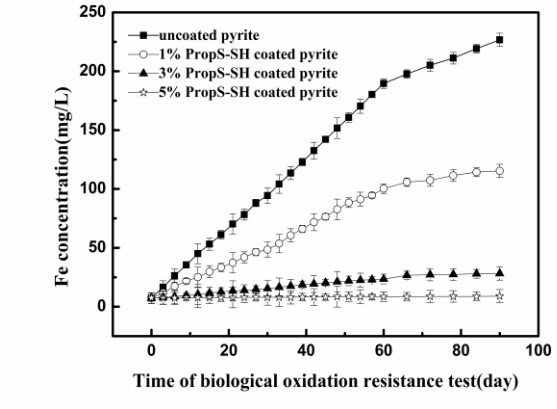

Figure 4. Release of Fe as a function of time for uncoated,1% , 3% and 5% PropS-SH coated pyrite samples in the bioleaching tests. (30℃,150 rpm, pH=2)

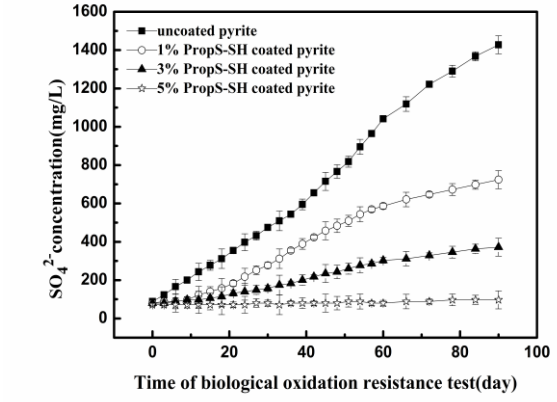

Figure 5. Release of SO_4^{2-} as a function of time for uncoated, 1% , 3% and 5% PropS-SH coated pyrite samples in the bioleaching tests (30℃,150 rpm, pH=2) .

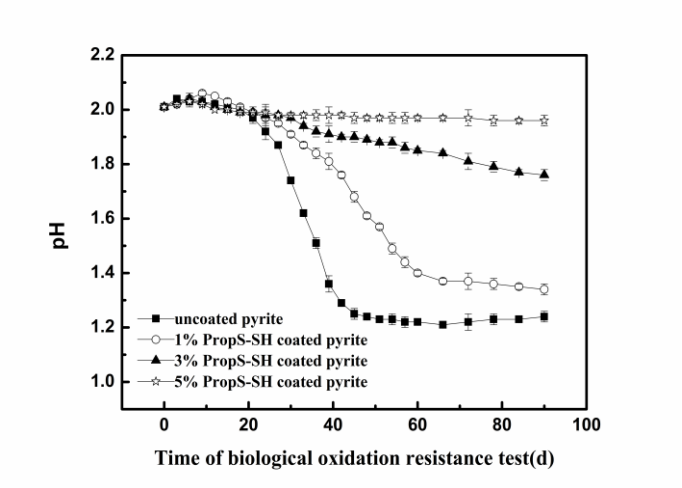

Figure 6. The solution pH at different time in the bioleaching tests (30℃,150 rpm) .

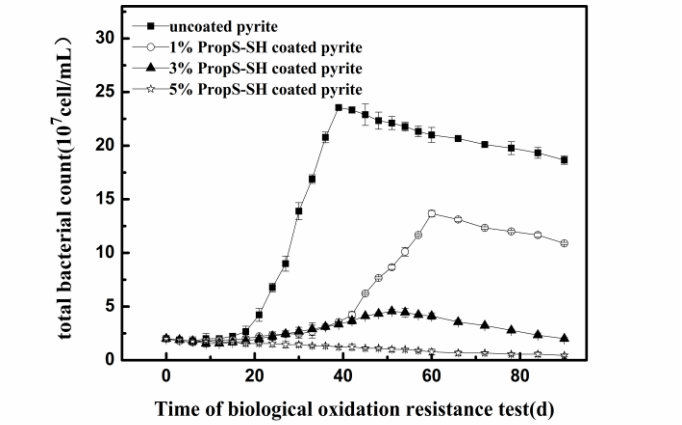

Figure 7. Bacterial growth curves in the bioleaching tests (30℃,150 rpm, pH=2) .

A biological leaching test was conducted to investigate the effectiveness of PropS-SH coating on pyrite in a simulated weathering environment, with the results shown in Fig.4 to 7 Obviously, the PropS-SH coating is able to reduce the biological oxidation of pyrite to a lower extent, as indicated by a comparison of the total Fe and SO_4^{2-} release, the pH change and the bacteria growth.

The concentrations of total Fe and SO_4^{2-} released into solution from bare pyrite increased markedly during the 90 day test (Fig.4 and Fig.5), reaching values of 226.7 and 1427.7mg/L. In comparison, the total Fe released from pyrite coated with 1%, 3% and 5% PropS-SH is decreased by 49.1%, 87.6% and 96.0%, respectively, and the SO_4^{2-} concentration in corresponding solution is reduced by 49.3%, 73.9% and 93.2% , respectively. In the biological leaching test, the decrease of pH values is observed for each treatment (as shown in Fig.6). By comparison, the decrease is highest in the uncoated pyrite, declining from an initial value of 2.00 to 1.19 in 90 days. While the pH decrease of 1%, 3% and 5% PropS-SH coated pyrite is from 2.00 to 1.35, 1.81 and 1.96, respectively, confirming that the inhibition efficiency increases with increasing PropS-SH concentration.

From the prior reports, it can be found that many passivating agents have been shown a certain degree of success in controlling iron sulfide oxidation. It was reported that acetyl acetone, sodium silicate and oxalic were able to reduce pyrite oxidation by 53% , 55% and 58%, respectively[Inhibition of pyrite oxidation by surface treatment]. The study of Elsetinow et al.[Suppression of pyrite oxidation in acidic aqueous environments using lipids having two hydrophobic tails] showed that the rate of pyrite oxidation under pH2 could be reduced by as much as 80% by treating pyrite with lipids having two hydrocarbon tails. At pH from 3.0 to 5.0 and temperature from 10–40°C, the amount of SO_4^{2-} leached out by 0.10 M H_2O_2 from the coated pyrite samples treated by 0.10 M H_2O_2/0.0034 M 8-hydroxyquinoline solution was 54.8–70.1% less than that from the uncoated pyrite [15]. Recenctly, Diao et al.[24] had found that tetraethylorthosilicate (TEOS) and n-propyltrimethoxysilane could reduce biological oxidation of pyrite by as much as 69 and 95% (based on Fe release), respectively, but the concentrations of these coating agents are unclear. Our previous research also showed that 5% TETA could reduce pyrite oxidation by 80.98%[16].

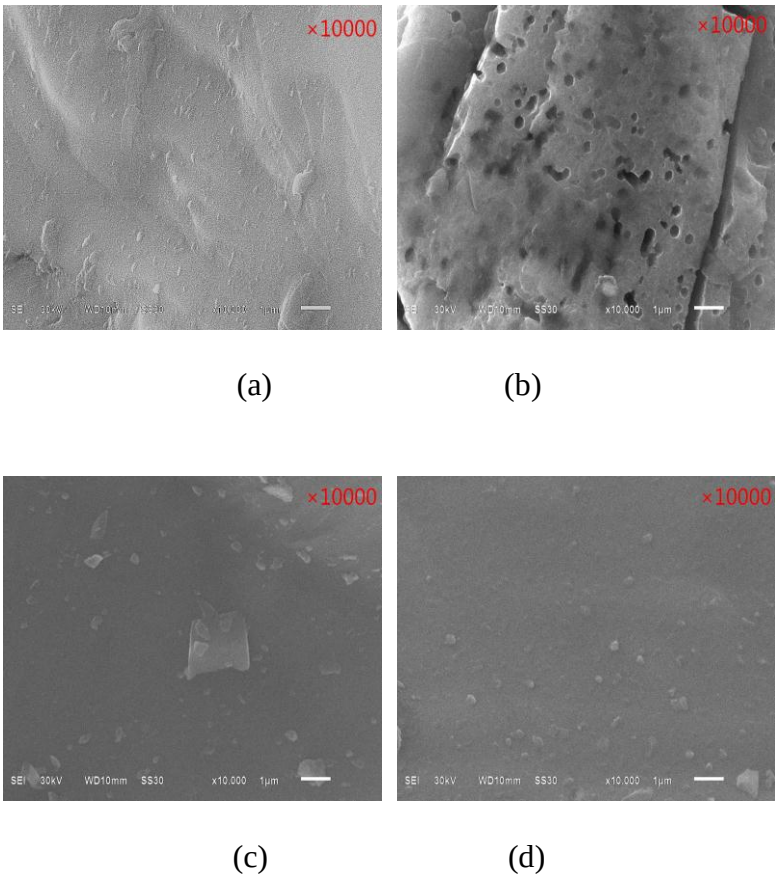

Figure 8. SEM images of uncoated/coated pyrite before and after the bioleaching tests. (a)Before biological oxidation(uncoated pyrite); (b)After biological oxidation(uncoated pyrite); (c)Before biological oxidation(5% PropS-SH coated); (d)After biological oxidation(5%PropS-SH coated).

However, the present study shows that the total Fe released from pyrite coated with 5% PropS-

SH can be decreased by 96.0%. By contrasting these results, we can know that PropS-SH is an efficiency passivating agent to reduce pyrite oxidation. What's more important, the use of PropS-SH coating needn't pretreatment of pyrite with hydrogen peroxide. The effect of PropS-SH coating on the growth of *Acidithiobacillus ferrooxidans* is illustrated in Fig.7. In the uncoated pyrite medium a short initial lag phase (18 days) in microbial growth is observed, continuing through exponential phase to 39 days where the highest cell number reached is 2.4×10^8 cells ml^{-1}. An increase in lag periods and a decrease in maximum cell numbers can be found in coated pyrite mediums. The maximum cell number in the coated pyrite mediums with 1% and 2% PropS-SH is decreased to 1.3×10^8 cells ml^{-1} and 4.9×10^7 cells ml^{-1}respectivly. When 5% PropS-SH coated pyrite is added in the culture medium, no visible growth of *Acidithiobacillus ferrooxidans* is observed. These results indicate the PropS-SH coating can prevent the contact of *Acidithiobacillus ferrooxidans* cells with pyrite and consequently inhibit the growth of bacteria.

The protection of pyrite from bacteria attack by PropS-SH can be further confirmed by SEM analysis, in which the uncoated pyrite and coated pyrite with 5% PropS-SH were selected for comparison (Fig.8). The surface of uncoated pyrite after the test is dotted with etch pits caused typically by the erosion of the bacteria, while the PropS-SH coating protected pyrite from oxidation, as no erosion was observed.

3.3 Characterization of the uncoated and coated pyrite samples

In order to better understand the role of PropS-SH on pyrite passivation, the surface chemical composition and wetting property of pyrite before and after different concentrations of PropS-SH treatment were characterized by XPS and Contact angle measurements.

3.3.1. XPS measurements

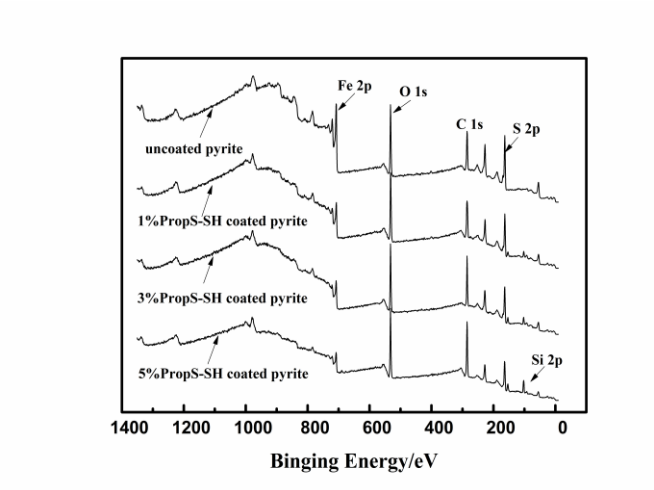

Figure 9. The complete XPS spectroscopy of uncoated pyrite and pyrite samples coated by different concentrations of PropS-SH.

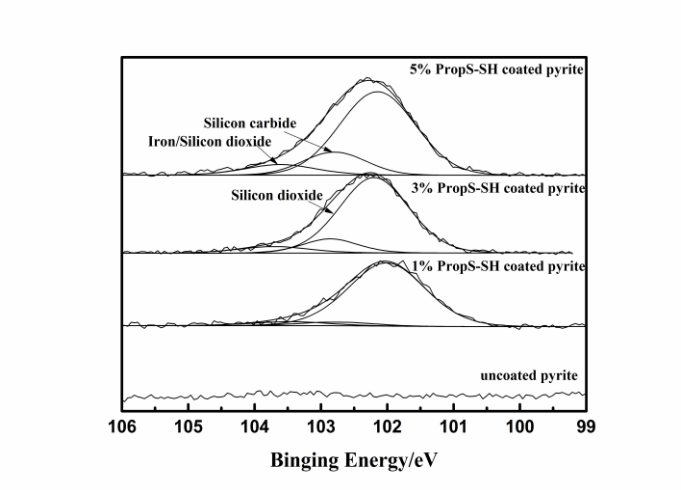

Figure 10. The Si 2p peak on the uncoated pyrite and pyrite samples coated by different concentrations of PropS-SH.

Fig. 9 displays the complete XPS spectra of pyrite before and after coating with various concentrations of PropS-SH. It can be seen that the signals of Si2p at around 102 eV and C1s at around 285 eV increase with an increase in PropS-SH concentration. After coating of PropS-SH on the surface of pyrite, the signals of Fe2p and S2p are obviously decreased. These results indicate that the higher concentration of the coating agent, the larger surface of pyrite has been covered.

The Si 2p spectra for uncoated and coated pyrite samples are compared in Fig. 10. Silicon is not detected on the uncoated pyrite but could be found in all of the coated pyrite samples. In the spectra of PropS-SH coated pyrite, The peaks around 102.10 and 102.80 eV are attributed to silicon dioxide and silicon carbide, respectively. The interaction between pyrite and coating agent is shown by the appearance of the peak recorded at 103.50 eV and its intensity increases with the PropS-SH concentration. This peak is in accord with iron/silicon dioxide, indicating Fe–O–Si bonds have been formed on the surface of pyrite. Chemical adhesion of PropS-SH on the surface of pyrite could be used to express the formation of a protective film.

3.3.2. Contact angle measurements

Contact angle measurements were conducted to assess the surface properties of uncoated and coated pyrite samples.

As can be seen from Fig.11, the contact angle of pyrite is increased with increasing PropS-SH content. the measured contact angle of the uncoated pyrite is only 54.56°and the corresponding values of 1%, 3% and 5% PropS-SH coated pyrite are 58.89°, 72.12°and 95.77°, respectively. Therefore it can be stated that coating with PropS-SH increases hydrophobicity of pyrite surface, thus resulting in a decreased interaction between pyrite and *Acidithiobacillus ferrooxidans* cells.

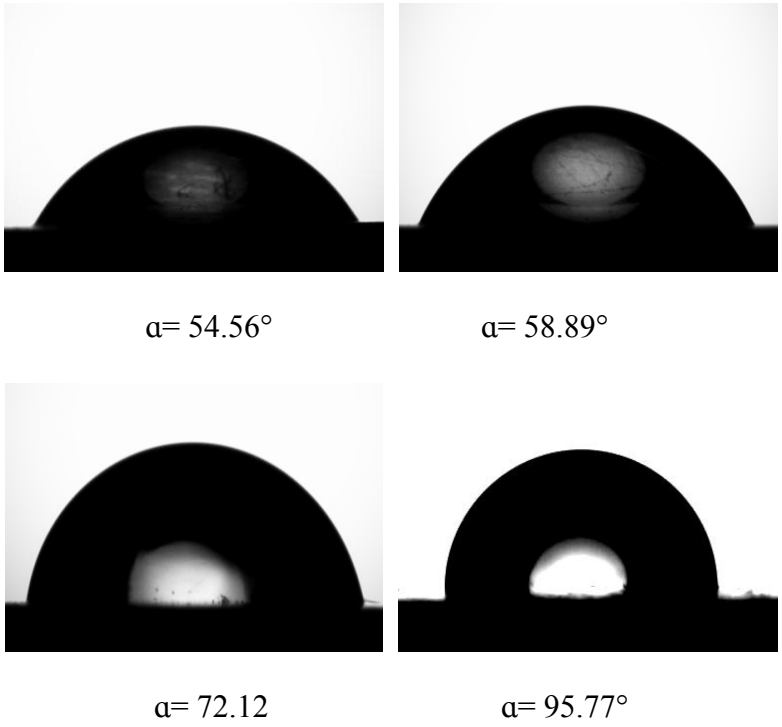

Figure 11. Contact angles of water droplets on pyrite samples coated by different concentrations of PropS-SH.

4. CONCLUSIONS

The feasibility of using PropS-SH coating to suppress biological oxidation of pyrite has been investigated in this study. The electrochemical tests show that the application of PropS-SH significantly decreases electrochemical activity of pyrite in bioleaching solutions and the inhibition efficiency is more pronounced with PropS-SH concentration. Release of S and Fe species and decreases in pH and microbial growth in the microbially mediated dissolution of pyrite are effectively suppressed in the presence of more than 5% of PropS-SH. PropS-SH coating suppresses the rate of biological pyrite oxidation by making the pyrite surface highly hydrophobic. The hydrophobic surface repels the bacteria attack, thus reducing the rate of oxidation of the treated pyrite. The results indicate that PropS-SH coating is useful for control of acid mine drainage.

References

1. Y. Liu, Z. Dang, P.X. Wu, J. Lu, X.H. Shu and L.C. Zheng, *Ionics*, 17(2010)169.
2. M. Gleisner, R.B. Herbert and P.C.F. Kockum, *Chemical Geology*, 225(2006)16.
3. A. Hierro, M. Olias, M.E. Ketterer, F. Vaca, J. Borrego, C.R. Canovas and J.P. Bolivar, *Environ Sci Pollut Res Int*, 21(2014)2611.
4. H.B. Zhao, J. Wang, W.Q. Qin, M.H. Hu and G.Z. Qiu, *Int. J. Electrochem. Sci*, 10(2015)848.

5. J.S. Lee and H.T. Chon, *Journal of Geochemical Exploration*, 88(2006)37.
6. D. Bejan and N.J. Bunce, *Journal of Applied Electrochemistry*, 2015(2015)1.
7. M.A. Caraballo, T.S. Rötting, F. Macías, J.M. Nieto and C. Ayora, *Applied Geochemistry*, 24(2009)2301.
8. A.L. Mackie and M.E. Walsh, *Water Res*, 46(2012)327.
9. A.R. Elsetnow , M.A.A. Schoonen and D.R. Strongin, *Environ. Sci. Technol*, 35(2001)2252.
10. C.Q. Xiao, R.A. Chi and Y.J. Fang, *Transactions of Nonferrous Metals Society of China*, 23(2013)2153.
11. D.M. Kargbo and S. Chatterjee, *Journal of Environment Engineering*, 131(2005)1340.
12. X. Zhang, M.J. Borda, M.A. A. Schoonen and D. R. Strongin, *Langmuir*, 19(2003)8787.
13. J. Hao, R. Murphy, E. Lim, M.A.A. Schoonen and D.R. Strongin, *Geochimica et Cosmochimica Acta*, 73(2009)4111.
14. P. Ačai, E. Sorrenti, T. Gorner, M. Polakovič, M. Kongolo and P. De Donato, *Colloids and Surfaces A: Physicochemical and Engineering Aspects*, 337(2009)39.
15. Y. Lan, X. Huang and B. Deng, *Arch Environ Contam Toxicol*, 43(2002)168.
16. Y. Liu, Z. Dang, Y. Xu and T.Y. Xu, *J Anal Methods Chem*,2 013(2013)1.
17. Y.W. Chen, Y. Li, M.F. Cai, N. Belzile and Z. Dang, *Minerals Engineering*, 19(2006)19.
18. X.H. Shu, Z. Dang, Q. Zhang, X.Y. Yi, G.N. Lu, C.L. Guo and C. Yang, *Minerals Engineering*, 42(2013)36.
19. Y.T. Ouyang, Y. Liu, R.L. Zhu, F. Ge, T.Y. Xu, Z. Luo and L.B. Liang, *Minerals Engineering*, 72(2015)57.
20. Y. Liu, Z. Dang, G.N. Lu, P. X. Wu, C.H. Feng and X.Y. Yi, *Minerals Engineering*, 24(2011)833.
21. B.F. Giannetti, S.H. Bonilla , C.F. Zinola and T. Rabóczkay, *Hydrometallurgy*, 60(2001)41.
22. H.Q. Fan, S.Y. Li, Z.C. Zhao, H. Wang, Z.C. Shi and L. Zhang, *Corrosion Science*, 53(2011)4273.
23. C. Liu, Q. Bi and A. Matthews, *Corrosion Science*, 43(2001)1953.
24. Z.H. Diao, T.L. Shi, S.Z. Wang, X.F. Huang, T. Zhang, Y.T. Tang, X.Y. Zhang and R.L. Qiu, *Water Res*, 47(2013)4391.